Research Paper

North Atlantic forcing of Indian Winter Monsoon intensification: Evidence from Holocene sediments from the tropical Indian Ocean Island of Sri Lanka

Kusala Madhushani Premaratne,[1,2] Rohana Chandrajith,[1] (iD)
Nalin P Ratnayake,[3] Si-Liang Li,[4] Kasun Gayantha[5,6]
and Joyanto Routh[7] (iD)

Abstract
The teleconnection between the Asian monsoon system and North Atlantic forcing is an enduring prospect of the Earth's climate. During the Holocene interstadial, the Indian summer monsoon showed asynchronous weakening links to ice rafting events documented in the North Atlantic region. However, the sensitivity of the Indian Winter Monsoon in response to North Atlantic cold spells is unclear due to a lack of compelling evidence. This study aims to extract the deglacial Indian Winter Monsoon signals using lithogenic tracers in coastal sediments and explore its association with the North Atlantic cooling episodes. A 5.1 m sediment core was retrieved from Pottuvil Lagoon in the southeastern coast of Sri Lanka, and the concentrations of K, Rb, Mg, Al, and Ti in 101 sub-sections were analysed using ICP-MS. The core- chronology was established by Bacon 2.2 age-depth modelling based on calibrated AMS ^{14}C dates. The monsoon signal was reconstructed using element proxies and compared with the drift ice indices from the North Atlantic deep-sea sediments. Results revealed distinct phases of intense monsoon activity at 2553–2984 years BP, 3899–5021 years BP, and 5244–5507 years BP intervals with intermittent weak phases during 2253–2553, 2984–3899, and 5021–5244 years BP. The episodes of the intensified Indian Winter Monsoon coincided with Bond Events 2, 3, and 4, showing a strong coherence with the North Atlantic's deglacial climate. Thus, on a millennial scale, North-Atlantic cooling has triggered intense winter monsoon conditions over the tropical Indian Ocean region from the mid to late Holocene. In comparison with regional monsoon archives, the Pottuvil winter monsoon record exhibits an anti-phase association with the Indian Summer Monsoon during Holocene ice-rafted debris events. The geochemical approach executed in this study could provide new insight into the millennial-scale pacing of the winter counterpart of the Indian monsoon links to climate extremes of high northern latitudes.

Introduction

The teleconnection between the Asian Monsoon and North-Atlantic climate is a well-documented expression in the glacial and Holocene environments of the Earth (Mohtadi et al., 2014). In particular, marine sediments (Deplazes et al., 2013; Gupta et al., 2003), speleothems (Band et al., 2018; Liu et al., 2013; Wang et al., 2005a), peat sequences (Rawat et al., 2015), loess deposits (Liu et al., 2020b), from the Asian monsoon region provide strong evidence on North-Atlantic forcing of the Indian and East-Asian monsoons.

Considering the last interglacial period, numerous paleo-monsoon records from the Asian monsoon domain have revealed marked changes in response to a quasi-periodic, '1500 years cycle' detected by Gerald Bond and his team (Bond et al., 1997) based on North-Atlantic deep-sea sediments. They used three proxies in sea bed deposits –the percentage of lithic grains, fresh volcanic glasses and haematite-stained grains to infer ice-rafted debris (IRD) events. These petrologic tracers detected peak IRD activity at around 1400, 2800, 4300, 5900, 8200, 9500, 10,300 and 11,000 years BP, showing different pacing on a millennial scale with a recurrence interval of

about 1500 years. Later, this millennial-scale cyclicity was detected in North-Atlantic's Holocene climate was called 'Bond Events' and considered counterparts of Pleistocene Dansgaard-Oeschger (D-O) events (Alley and Agustsdottir, 2005).

[1]Department of Geology, Faculty of Science, University of Peradeniya, Sri Lanka
[2]Department of Marine Chemistry, Leibniz Institute for Baltic Sea Research, Germany
[3]Department of Earth Resources Engineering, Faculty of Engineering, University of Moratuwa, Sri Lanka
[4]Institute of Surface-Earth System Science, School of Earth System Science, Tianjin University, China
[5]Max-Planck Institute of Biogeochemistry, Germany
[6]Thermo Fisher Scientific, Germany
[7]Department of Thematic Studies – Environmental Change, Linköping University, Sweden

Corresponding author:
Rohana Chandrajith, Department of Geology, Faculty of Science, University of Peradeniya, Peradeniya 20400, Sri Lanka.
Email: rohanac@pdn.ac.lk

Notably, both the Indian Summer Monsoon (ISM) and East Asian Summer Monsoon (EASM) have significantly weakened through the intervals of increased ice rafting activity recorded in North Atlantic deep-sea sediments during the Holocene. In the Indian monsoon domain, for instance, weakened ISM in response to the 8.2 Bond event was well-documented in the Arabian Sea (Gupta et al., 2003), NW Himalaya (Rawat et al., 2015), Central India (Band et al., 2018). In addition, 0.5 ka Bond Event (the Little Ice Age), 1.4 ka event (the Dark Age cold period), 2.8, 4.2, 5.5, 9.4 and 10.3 ka events were detected as periods of declined ISM activity (Band et al., 2018; Gupta et al., 2003; Rawat et al., 2015). Similarly, as evidenced in southern, western and central China, North-Atlantic cold spells left their signature as weakened EASM (Liu et al., 2013, 2020a; Wang et al., 2005b). In these paleoclimate records, the signal of weakened summer monsoon has been inferred by decreased abundance of *G. bulloides* in marine sediments (Gupta et al., 2003), increased $\delta^{18}O$ values or asynchronous increase of ^{18}O and Mg/Ca values in spelaeothem carbonates (Band et al., 2018; Liu et al., 2013; Wang et al., 2005a), low total organic carbon (TOC) values along with increased $\delta^{13}C$ and decreased pollen assemblages in peat sequence (Rawat et al., 2015) and by elemental proxies Rb/Sr and Zr/Rb in loess deposits (Liu et al., 2020b).

In contrast, several studies have shown an asynchronous intensification of the East Asian Winter Monsoon (EAWM) during Holocene IRD events (Hao et al., 2017; Hu et al., 2012). In particular, strong EAWM events recorded in grain size proxy of Central Yellow Sea Mud, China (Hu et al., 2012), terrestrial lignin phenols from South Yellow Sea, China (Hao et al., 2017) and elemental proxies Rb/Sr and Zr/Rb in loess deposits from Western China (Liu et al., 2020a) are well correlated with Bond events 0–5, 0–4 and with 2–8 respectively. Accordingly, on the centennial to millennial scale, EASM and EAWM exhibit an inverse-phase relationship linked to North-Atlantic cooling since the last glacial period (Henry et al., 2016; Liu et al., 2020a). However, the sensitivity of the winter counterpart of the Indian monsoon in association with North Atlantic cold spells is still elusive to the present knowledge due to a lack of comprehensive evidence. In such circumstances, this study aims to reconstruct the deglacial Indian Winter Monsoon signals and its tele-connective response during Holocene IRD events based on sedimentary archives from Sri Lanka- an Island located in the core of the Indian monsoon domain.

In chasing the Holocene monsoon, Sri Lanka provides an excellent repository, owing to its unique geographical position in the Indian monsoon domain. Sri Lanka is affected by both summer and winter monsoon circulation as it lies directly in the monsoon trajectory across the Indian Ocean (Figure 1), thus having a classic tropical monsoon climate. During Boreal summer, the atmospheric pressure gradient across the warm Tibetan Plateau and cooler Indian Ocean causes south-westerly winds, which bring summer rainfall over the Indian Ocean and southern and south-west regions of the Asian continent (Rashid et al., 2007). This is known as the Indian Summer Monsoon (ISM) or Southwest Monsoon (SWM). In May, summer rainfall is triggered across Sri Lanka as the Inter-Tropical Convergence Zone (ITCZ) crosses the island during its northerly displacement. The mid-tropospheric wind movements, that is, cyclonic circulations, cause heavy rains primarily across southwestern parts of the island during the summer months. Due to the orographic effect, the highest summer rainfall lies on the western slopes of the central highlands (Figure 1). Summer monsoon fades in Sri Lanka in September when the ITCZ moves towards the south. In September, the high-pressure zone over the cooler north Indian landmass and the low atmospheric pressure over the warmer Indian Ocean generate north-easterly winds that blow from the Himalayas and Indo-Gangetic Plain towards the Indian Ocean (Rajmanickam et al., 2017). This is referred to as the Indian Winter Monsoon (IWM) or Northeast Monsoon (NEM). The
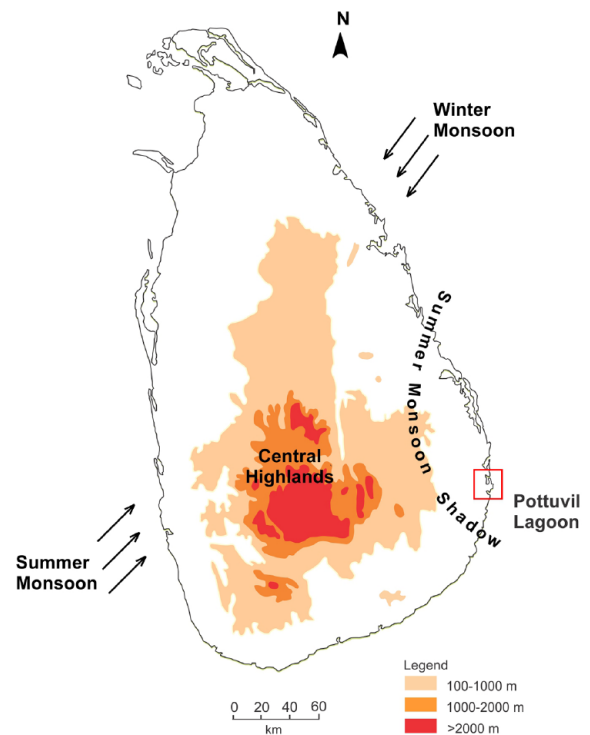

Figure 1. Geomorphology of Sri Lanka (modified after Chandrajith, 2020) and orographic effect of Central Highlands. The elevated landscape above 1000 m makes up the central mountains of the island.

winter rainfall hits Sri Lanka in December as ITCZ crosses the Island in its' southerly migration. During the northern hemisphere winter, the specific circulation conditions in the easterly wind stream and cyclonic wind circulations of the mid-troposphere bring heavy rainfall to the eastern half of Sri Lanka. In particular, the eastern slopes of the highlands receive the highest winter rainfall, owing to the orography of the Island. The winter monsoon season in Sri Lanka usually lasts until around February.

The southeastern coastal lowlands of Sri Lanka serve as an excellent archive of Indian winter monsoon variability because the area is influenced by the dominant winter monsoon variant and is shielded by summer rainfall. The central highlands of Sri Lanka, with a maximum height of about 2400 m, obstruct the propagation of summer monsoon winds towards the eastern terrain, creating a rain shadow around the east-southeast parts of the Island (Figure 1). Thus, paleoclimate records from the east-southeast parts of the island predominantly represent the winter monsoon signatures. Further, sedimentary deposits from coastal lagoons in this region enable paleoclimate investigations spanning the Holocene, as the lagoons are thought to have resulted from the late Quaternary marine transgression and sea-level rise (Silva et al., 2013). In this context, we used an AMS ^{14}C dated sediment core from the Pottuvil lagoon in south-eastern Sri Lanka to trace the Indian winter monsoon variability and its association with North Atlantic cooling episodes during the Holocene.

Reconstruction of the monsoon signal was based on lithogenic proxies of sediments. This study used K, Rb, Mg, Al, and Ti as indicators of terrigenous detrital flux (monsoonal discharge) to the lagoon. These elements have been widely used as monsoon proxies, which reflect the responses of the catchment to changing climate (Achyuthan et al., 2014; Bhushan et al., 2018; Gayantha et al., 2017; Ning et al., 2017). Monsoon dynamics could be traced with reference to rainfall intensity and/or the amount of precipitation, rates or intensity of chemical weathering and erosion in the catchment, surface runoff from local watersheds, and fluvial discharge based on detrital elements such as Al, K, Rb, Mg
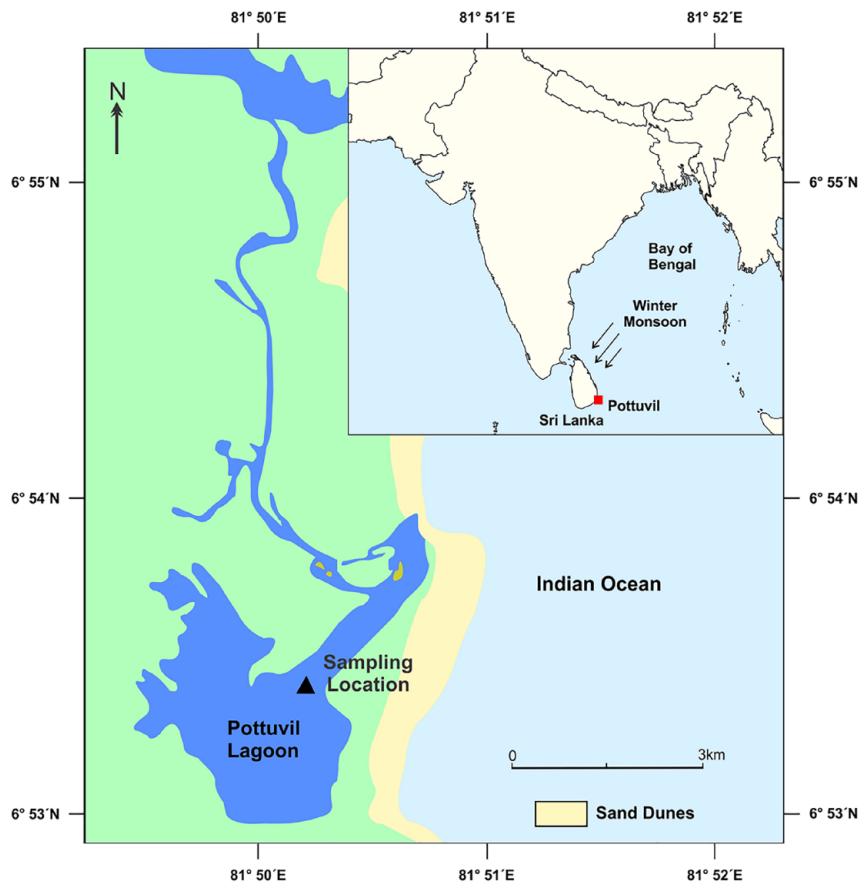
Figure 2. Location of Pottuvil Lagoon in the southeastern coastal plain of Sri Lanka and the sampling location.

(Gayantha et al., 2017; Lone et al., 2018; Ning et al., 2017). In addition, detrital Ti is frequently used as a proxy for catchment erosion driven by climate (Ning et al., 2017). The Ti-bearing minerals are highly resistant to weathering and are considered a refractory element in surface environments (Chen et al., 2020). Since Sri Lanka has a classic tropical monsoon climate due to its unique geographical position in the Indian monsoon domain, we surmise that the lithogenic proxies in Pottuvil lagoon sediments might be closely reflected in induced changes.

Material and methods

Study area

Pottuvil Lagoon is a brackish-water lagoon located in the Ampara District of the Eastern Province of Sri Lanka (Figure 2), which covers an area of about 25 km^2 in south-eastern coastal lowlands. It is connected to the sea on its eastern border by a 170 m-long narrow channel. The lagoon was formed by back-barrier formation along the southeastern coast during the Holocene (Silva et al., 2013). Located in the dry zone of Sri Lanka, the mean annual temperature and precipitation around the Pottuvil area are 27.4°C and 700–1000 mm, respectively. The lagoon receives freshwater mainly from direct winter (northeast) monsoon precipitation from December to February. During the summer months, the Pottuvil coastal stretch experiences an arid climate. At present, monthly total rainfall around Pottuvil during the May-September period is as low as 50 mm, and from December to February, monthly total rainfall exceeds 250 mm. Therefore, the area is influenced by the dominant winter monsoon variant. In addition, the Pottuvil lagoon is also fed by several perennial streams, while tidal fluctuations affect the lagoon, and the salinity can be over 30‰, depending on the season. Pottuvil Lagoon has a watershed of about 479 km^{2}i, entirely underlain by

crystalline, high-grade metamorphic rocks. The southeastern coastal sector is underlain by amphibolite-facies rocks rich in hornblende and biotite. These basement rocks and outcrops in this area have been weathered and configured on the island during Holocene submergence (Silva et al., 2013).

Sediment core collection

Coring was carried out in the Pottuvil Lagoon using a mechanically driven piston corer fixed in a floating barge. The piston coring method extracts sediments with minimum disturbances to the recovered sample. The sampling location (6° 53′ 27″N; 81° 50′ 18″E) was selected by considering the deepest point of the lagoon (Figure 2). The drilling depth was approximately 5.2 m, and the core was acquired into polyvinylchloride (PVC) tubes with 6.5 cm diameter. The core was sliced at 1.0 cm, and geochemical analysis was carried out for sub-samples selected at a 5 cm interval.

Age-depth modelling

Bulk organic carbon in sediments and mollusc shells extracted from the core were analysed for ^{14}C ages to construct the age-depth model for the Pottuvil sediment core. Altogether, five bulk dates and one shell date were used to establish the chronology. The entire core was dominated by terrestrial sediment input. Hence, we used five ^{14}C ages derived from bulk organic carbon in sediments, representing the core. The bulk sediment samples were pre-treated to remove the inorganic content, so we used only the bulk organic carbon fraction for ^{14}C dating (Table 1). Radiocarbon analysis was performed using an Accelerator Mass Spectrometer (AMS) at the Radiocarbon Laboratory, Max Planck Institute of Biogeochemistry, Jena, Germany and Institute of Surface Earth System Science (ISESS), Tianjin University, China, adapting the sample preparation method described by Steinhof

Table 1. AMS ^{14}C dates used to establish the chronology of the Pottuvil core.

Depth (cm)	Dating material	14C Age BP	Cal yr BP	Cal yr BP (95% CI)
10	Bulk organic carbon in sediment	2081 ± 15	2287	2077–2874
100	Bulk organic carbon in sediment	2982 ± 49	3130	2962–3336
210	Bulk organic carbon in sediment	3664 ± 15	3943	3850–4061
310	Bulk organic carbon in sediment	4741 ± 16	4498	4319–4666
385	Shell	4773 ± 19	4854	4694–5046
502	Bulk organic carbon in sediment	4858 ± 46	5517	5336–5672

et al. (2017). Further, the mollusc shell used for the age dating was extracted from the 340 to 420 cm depth section of the core, where shells and shell fragments are mainly abundant. The age-depth model of the core was established using the R-software package BACON (r-bacon), which uses Bayesian statistics to construct the sediment chronology (Blaauw and Christen, 2011). In this approach, the core is divided into vertical sections, and the accumulation rate (in years/cm) for each section is estimated through Markov Chain Monte Carlo (MCMC) iterations. Combined with an estimated starting date for the first section, the accumulation rates for the individual sections give the age-depth model (Blaauw and Christen, 2011). All the bulk (organic) ^{14}C dates were calibrated using the Northern Hemisphere Terrestrial Calibration Curve (IntCal20). Due to possible marine influence in the lagoon, the mollusc shell date was calibrated using the Northern Hemisphere Marine Calibration Curve (MarineCal20) (Reimer et al., 2013). It was corrected for the reservoir age effect. We used 133 ± 65 as the local marine reservoir age, according to the online Marine Reservoir Database (http://calib.org/marine/).

Grain size analysis

Grain size analysis was conducted for sediment samples selected at 5 cm intervals. About 1.5 g wet bulk sample was pre-treated with 30% HCl and 30% H_2O_2, and sodium hexametaphosphate (0.05%) was used as the wet dispersant for particle size analysis. Pre-treated samples were sonicated in an ultrasonic stirrer for 1–2 min and then introduced to a Laser Diffraction Particle Size Analyzer (Malvern Mastersizer 3000) through a Hydro LV wet sample dispersion unit. The results were expressed as weight percentages of sand, silt and clay.

Geochemical analyses

Approximately 100 mg of dried and powdered samples were digested at 180°C using 3: 1 ratio of 65% nitric acid (Merck Suprapur®) and 30% hydrochloric acid (Fluka TraceSELECT®) in a microwave reaction system (CEM- MARS-6) equipped with Easy-Prep + high-pressure vessel system. In samples, K, Rb, Mg, Al, and Ti were quantified using an Inductively Coupled Plasma Mass Spectrometer (ICP-MS; Thermo ICapQ). For the ICP-MS analysis, we used a five-point calibration curve based on certified NIST traceable ICP grade stock solutions. The instrumental drift was checked with the ^{21}Sc (1.0 μg/L) internal standard, and the method validation was performed using certified reference materials (CRM).

Signal processing and statistical analyses

Signal processing and statistical analyses were carried out using Microcal Origin Ver. 7 for Windows. The fast Fourier transform (FFT) filter facility of the 'Signal Processing' package in Origin was used to acquire a smoothed signal from the original data. The FFT low pass filter removes high-frequency noises from the signal, which helps identify long-term fluctuations in data. In this study, Fourier transformed Low Pass fit filter was applied on each proxy (K_2O, Rb_2O, MgO, Al_2O_3 and TiO_2) with a cut-off frequency of 0.0245 Hz for depth variations and 0.0037 Hz for time
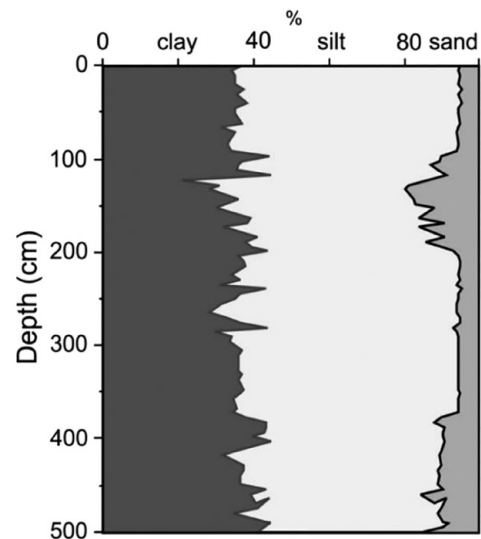
Figure 3. Variation of sand, silt, and clay (%) in the Pottuvil sediment core.

series. The cut-off frequencies were selected by granting the minimum distortion of the original signal. In the FFT low pass filter, the frequencies higher than the cut-off frequency were discarded from the signal. The filtered values were plotted in 2D graphical format and superimposed on the original signal for better visualisation of the results.

The time series of oxide contents in the sediment core was compared with the Hematite Stained Grains (HSG) record of the North Atlantic deep-sea core MC52-VM29-191 (Bond et al., 2001). In the HSG record, cold events were indicated by high percentages of hematite-stained grains in sediments (Bond et al., 2001). The chronology of the Pottuvil core spans within the range of 2, 3, and 4 cold events detected in the MC52-VM29-191 core. Pearson's correlation analysis was performed to identify potential relationships among geogenic elements. All the correlations are significant at 0.01 level (2-tailed).

Results and discussion

Stratigraphy, grain size distribution and chronology

The Pottuvil sediment core was primarily composed of massive dark grey clay-rich layers with intermittent silt and sand layers of greyish to pale greyish colour. The silt and clay content of the core ranged from 40 to 60% and 30 to 50%, respectively, but sand content was relatively low (<14%) (Figure 3). Unbroken shells and shell fragments were scattered throughout the core. In particular, large intact shells were more abundant in the 340–420 cm depth section. Macro shells in the core mainly were either gastropod (shell height; approx. 0.4–2.0 cm) or bivalve molluscs (shell width; approx. 0.3 cm to 2.3 cm). The sediments spanned from 5.5 (500 cm) to 2.2 (0 cm) kyr before the present (BP) (model median age) according to the BACON age-depth model (Figure 4). In this model, the surface layer
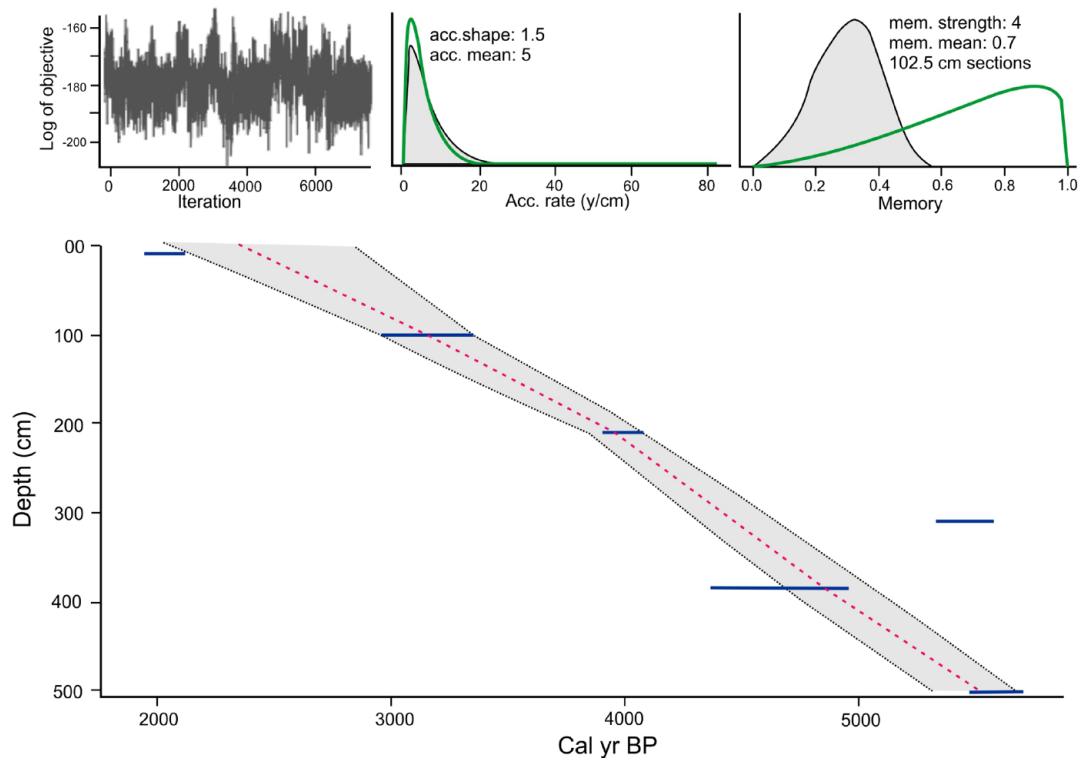
Figure 4. Age-depth model of the Pottuvil core profile based on Bacon 2.2 modelling routines (Blaauw and Christen, 2011). The dotted line shows modelled mean ages along the core, and the grey stippled lines indicate the 95% confidence intervals of the modelled age-depth relationship. Graph (a) shows the iteration history, and graphs (b and c) show prior (green lines) and posterior (grey histograms) density functions for accumulation rate and memory.

(0 cm) corresponds with an age of 2.2 kyr BP, indicating a possible hiatus in the depositional history of the last 2.2 kyr BP years. One possible reason for the missing record is the impact of the tsunami that has eroded the topmost sediment layers. In the most recent scenario, many parts of the coastal lowlands of Sri Lanka were affected by the 2004 trans-basin Indian Ocean Tsunami. However, the tsunami inundation and the impact along the coast differed, depending on the coastal geomorphology. Therefore, the washout signature of the top sediment layers may vary with the location of sediment coring. A similar depositional hiatus has been reported in sediments from Bolgoda South Lake, located on the southwest coast of Sri Lanka, in which the age-depth model was trimmed at ca. 1410 cal yr BP (Gayantha et al., 2020). The ^{14}C age of the shell date used for the age-depth model was corrected for the local marine reservoir age ($\Delta R = 133 \pm 65$).

Lithogenic proxies and reconstruction of monsoon signals

Paleo-monsoon reconstruction was based on the lithogenic proxies present in the Pottuvil lagoon sediments. In this study, K, Rb, Mg, Al and Ti were indicators of terrigenous detrital flux (monsoonal discharge) to the lagoon. Potassium, Rb and Mg can be expressed in the weight scale of each element or as oxide or either normalised to Al or Ti as depicted in many studies. Here, we present the content of K, Rb, Mg, Al and Ti as oxides (mg/kg). The concentrations of K_2O, Rb_2O, Al_2O_3, MgO and TiO_2 in the sediment core showed drastic fluctuations with the depth, ranging from 275 to 6063 mg/kg (average 3126), 4 to 89 mg/kg (average 33), 1576–35,585 mg/kg (average 16,848), 364–10,496 mg/kg (average 4671), and 96–1635 mg/kg (average 782), respectively. The Fourier transformed 0.0245 Hz low pass fit filter of each proxy is superimposed on the original signal for better visualisation of the results (Figure 5). Notable peaks with
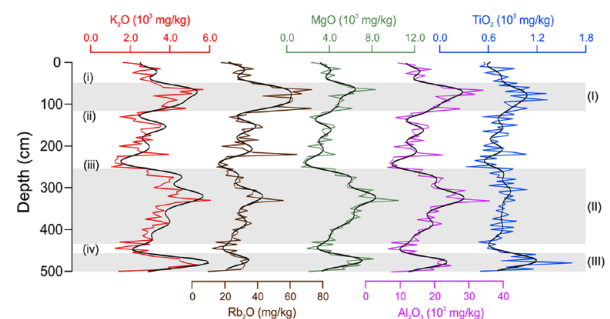

Figure 5. Depth variations of lithogenic oxide concentrations in Pottuvil sediments. The solid black line represents the Fourier transformed 0.0245 Hz low pass fit filter of each proxy. Three major events are denoted as (I), (II), and (III) (shaded), whereas it marked notable monsoon troughs in (i), (ii), (iii), and (iv).

increased levels of K_2O, Rb_2O, Al_2O_3, MgO, and TiO_2 were recorded around 48–116, 254–432, and 457–500 cm depth intervals of the core with corresponding age intervals of 2553–2984 years BP, 3899–5021 years BP, and 5244–5507 years BP. In 0–48 cm (2253–2553 years BP), 116–254 cm (2984–3899 years BP), and 435–457 cm (5021–5244 years BP) depth sections, oxide concentrations were relatively low. Further, the 116–254 cm section featured a series of troughs with smaller amplitudes extending from 2984 to 3173 years BP, 3255 to 3444 years BP, and 3690 to 3899 years BP. From 3899 to 2984 years BP, oxide contents were slightly increased.

The periods of increased lithogenic elements in Pottuvil sediments likely resulted from intense weathering and erosion in the catchment and subsequent enrichment in the detrital phase. In particular, each oxide strongly correlated with Al_2O_3 ($r = 0.97$ K_2O; $r = 0.78$ Rb_2O; $r = 0.92$ MgO; $r = 0.62$ TiO_2), suggesting their association with the terrigenous detrital flux to the

lagoon. Aluminium and Mg are primarily associated with clay minerals during weathering, and K is leached into the dissolved phase. However, K could also be incorporated into clay minerals. In addition, Rb is closely associated with K (Kabata-Pendias and Pendias, 1984). The weathered products containing detrital elements in either dissolved or solid phases were eventually transported to the lagoon. Chemical weathering is intense under a warm, humid climate, and high erosion in the catchment is favoured by enhanced surface runoff. Extreme rainfall triggers increased surface runoff and, thus, high fluvial discharge (Achyuthan et al., 2014; Lone et al., 2018; Ning et al., 2017). Elevated Al_2O_3, Rb_2O, and MgO levels in sediments indicate increased precipitation and surface runoff from the catchment into the lakes (Bhushan et al., 2018). Elevated values of K/Al and Mg/Al signify an increased rate of weathering and catchment instability attributed to warm, wet, and intense rainfall conditions (Gayantha et al., 2017). Titanium mainly occurs in detrital minerals associated with the terrigenous flux resulting from erosion in the watershed (Chen et al., 2020). Higher Ti/Al values in sediments indicate intense weathering in the catchment during a decisive monsoon phase (Gayantha et al., 2017, 2020). Increased Ti contents suggest a high allochthonous input in the drainage basin (Ning et al., 2017).

Pottuvil Lagoon receives freshwater mainly from direct precipitation from the Indian winter monsoon. In the Pottuvil core, K_2O, Rb_2O, Al_2O_3, MgO and TiO_2 also exhibited a statistically significant correlation with each other and parallel variations in depth profiles of each proxy, implying a similar source. Most notably, the depth profiles of oxides showed in-phase variations in both the original and the smoothed signals. Thus, the major peaks of lithogenic element contents could be attributed to warm, humid areas with intense rainfall and increased fluvial input to the lagoon. Amongst, 2553–2984 and 5244–5507 kyr BP peaks were short-lasting events, while the 3899–5021 kyr BP peak was a prolonged episode of intense monsoon activity. In contrast, troughs in oxide profiles would reflect suppressed or weak monsoon conditions. The troughs were paced at nearly 1300–1500 years intervals apart in the filtered signal, implying a distinct millennial-scale variability of the winter monsoon climate. Notably, the recurrence interval of major monsoon peaks was approximately 1000–1600 years.

Links to North Atlantic cold episodes

The temporal variations of the Pottuvil monsoon record were compared with drift ice indices, that is, Hematite Stained Grains (HSG) in the North Atlantic deep-sea sediments (core no. MC52-VM29-1914) (Bond et al., 2001). In the HSG record, cold events are indicated by higher percentages of hematite-stained grains and the 2.8 (B-2), 4.2 (B-3), and 5.9 (B-4) Bond events showed close association with the Pottuvil monsoon record. Each cold event was labelled as (a) and (b) doublets for visual correlation. Strong coherence was observed between the oxides and HSG time series in their general pattern and timing of the peaks and troughs in both original and smoothed monsoon signals. In particular, a close correspondence was revealed between drift ice indices and intensified episodes of winter monsoon recorded in Pottuvil sediments at B-4 (b), B-2 (a), and B-2 (b) events. During the 4.2 Bond event, the original signal of lithogenic proxies was closely linked with the B-03(a) peak (Figure 6).

Accordingly, the results revealed a strengthening of the Indian winter monsoon coeval to the intervals of increased ice rafting documented in the North Atlantic region (Bond et al., 1997). In addition, the major monsoon troughs also showed a parallel progression along with the HSG record. The in-phase relationship observed between the Pottuvil winter monsoon record and Bond events is unlikely to reveal a random coincidence; instead, it might reflect a mechanistic link operated on the millennial scale. Several convincing pieces of evidence were found in the winter monsoon
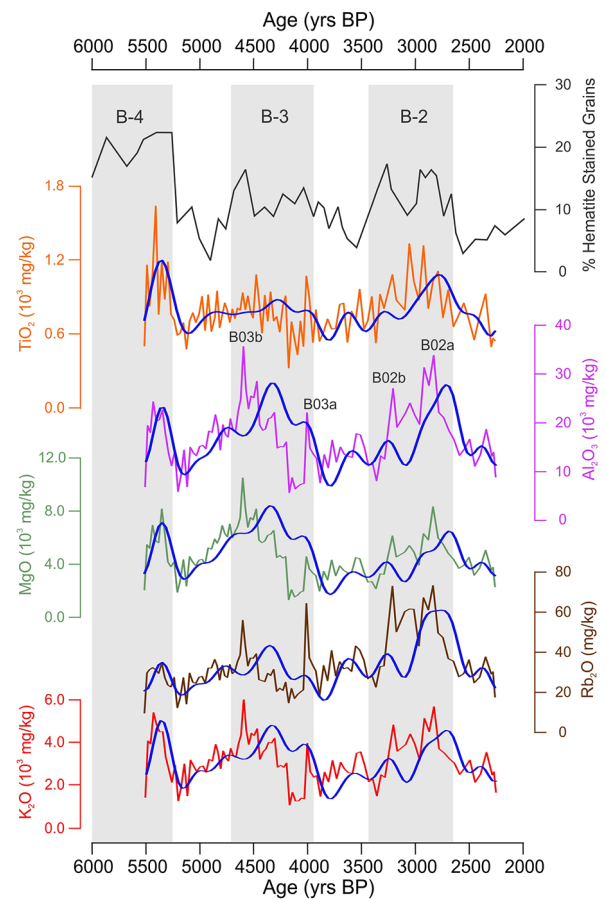

Figure 6. Variations of lithogenic tracers in the Pottuvil sediment core compared with Hematite Stained Grains (HSG) record of the North Atlantic deep-sea core MC52-VM29-1914. Major ice rafting events are denoted as B-2, B-3, and B-4 (shaded), in which higher percentages of HSG imply an elevated influx of ice-rafted debris and subsequently, referred to as cold events. The solid blue line represents the Fourier transformed 0.004 Hz low pass fit filter of each proxy. The B-2 and B-3 events appear to have doublets in lithogenic proxies, which are labelled as a and b.

records from many East Asian regions. In particular, monsoon signatures recorded in proxies such as total organic carbon (Yancheva et al., 2007), $\delta^{18}O$ (Sagawa et al., 2014), aeolian dust flux (Yu et al., 2011), Ti (Yancheva et al., 2007), and lignin proxies (Hao et al., 2017), revealed a notable association with timing and relative magnitude of Bond events from mid to late Holocene, implying the impact of North Atlantic cooling on the East Asian winter monsoon. Analogous to these observations, several studies show an intensification of East Asian winter monsoon during the intervals of increased ice rafting (Hao et al., 2017). Though comparable winter monsoon studies are rare from the Indian monsoon domain, paleoclimate archives from southern India (Mishra et al., 2019) and the north-eastern Arabian Sea (Lückge et al., 2001) provide clues on intensified IWM at around 0.5, 1.4, 2.8 and 4.4 ka BP. In these records, a strengthened monsoon signal was inferred as decreased FeO% in lake sediments (Mishra et al., 2019) and increased K/Al ratio of marine sediments (Lückge et al., 2001).

Further, the timing of peak IWM activity detected in both studies is closely in phase with B03(a & b) Bond events, based on visual correlation. However, the link between the Indian winter monsoon and North Atlantic cold snaps is less explored than that of the summer counterpart due to a lack of comprehensive evidence. Besides, most Indian summer monsoon records reveal an abrupt weakening in response to North Atlantic forcing (Band et al., 2018; Gupta et al., 2003; Rawat et al., 2015). Thus, this study provides a new insight into (a) the existence of a

teleconnection between the Indian winter monsoon and the North Atlantic climate and (b) an inverse phase climate response of Indian winter and summer monsoons during Holocene IRD events.

Reportedly, the cooler surface temperatures of the Indian Ocean played a crucial role in Indian monsoon failure during North Atlantic stadials (Pausata et al., 2011; Tierney et al., 2016). In a broad exposition, the tele-connective response of the Indian summer monsoon involves a coupled ocean-atmosphere mechanism in propagating the cooling signals from the North Atlantic and synchronised changes in tropical mean circulation patterns (Mohtadi et al., 2014). In particular, freshwater hosing experiments based on model simulations have shown a substantial deceleration in the Atlantic meridional overturning circulation and colder conditions in surface waters of the North Atlantic during Henrich-stadials and the Younger Dryas (Mohtadi et al., 2014). The atmospheric advection process rapidly transmitted this cooling signal through the northern hemisphere (Clement and Peterson, 2008). Consequently, anomalous energy flow was generated from the warm southern hemisphere to the anomalously cold northern hemisphere, signifying the response of tropical atmospheric circulation to cooling in the North (Mohtadi et al., 2014). The energy is transported through changes in the Hadley circulation in which upper and lower branches of the Hadley cell exhibit unusual northward and southward flows, respectively (Frierson et al., 2013). As a result, the rising branch of the Hadley cell shift southwards, leading to a dry climate over the equatorial and northern Indian Ocean and a humid climate towards the south (Mohtadi et al., 2014).

However, this mechanism does not explain how cooling in the north could trigger warm, wet monsoons over the equatorial latitudes during northern winters, as recorded in this study and several other shreds of evidence from the Indian monsoon domain. This observation is pointed towards the Indian winter and summer monsoons that most likely responded differently to the North Atlantic forcing. Nevertheless, compelling observations from the Indian monsoon realm are sparse. However, some studies based on East Asian monsoons exhibit contrasting responses to cooling in the north in summer and winter counterparts. For example, the East Asian winter monsoon was strong during cold episodes of the Heinrich event-1 and Younger Dryas, whereas the East Asian summer monsoon was weak during these cold events (Liu et al., 2020a). Model simulations further revealed that, on a millennial scale, North Atlantic cooling has resulted in an anti-phase relationship between East Asian summer and winter monsoons (Wen et al., 2016). The contrasting response of Indian summer and winter monsoons may have arisen from seasonal dissimilarities in the sensitivity of the tropical circulation to diabatic cooling and subsequent cross-hemispheric response. Solid evidence is observed from idealised modelling experiments that investigated the Hadley cell's response to localised forcing (Baker et al., 2018). In particular, Hadley cell exhibits seasonal-based, contrasting sensitivities to diabatic heating in a dry idealised atmospheric general circulation model.

Further, this model simulation has shown that heating triggers an interhemispheric response in the Hadley cell and, consequently, the jet stream. For example, strong associations were observed in the Hadley cell extent and jet dynamics in the winter (summer) hemisphere once the heating is forced from the summer (winter) hemisphere (Baker et al., 2018). The observed seasonal contrast in cross-hemispheric response to heating is governed by the influence of the dominant winter Hadley cell (Baker et al., 2018). The Hadley cell and eddy-driven jet are co-dependent (Previdi and Liepert, 2007), and this relationship varies seasonally (Ceppi and Hartmann, 2013). Furthermore, the Hadley cell variability is predominantly led by eddy-driven changes (Caballero, 2007).

Similarly, Hadley cell has shown seasonal sensitivities to forcing like the El Niño–southern oscillations and global warming (Baker et al., 2018). More investigations are needed to verify that diabatic cooling causes similar results in tropical atmospheric circulation. Thus, these findings peer into a broader perception that the teleconnective behaviour of north-Atlantic cooling and monsoonal response in summer and winter counterparts should be studied in comparison with each other to unravel the exact mechanism.

Conclusions

The geochemical approach executed in this study provides new evidence on distinct, millennial-scale pacing of the Indian winter monsoon variability during the last deglacial period. Further, those variations observed in the lithogenic proxy record, and thereby the intensified episodes of the Indian winter monsoon, were controlled by North Atlantic forcing. This adds to an emerging evidence that a mechanistic link exists between the North Atlantic climate and tropical atmospheric circulation in the the winter counterpart. Moreover, IWM showed an inverse phase climate response with ISM during Holocene IRD events. The mechanism by which North Atlantic forcing affects the Indian winter monsoon is unclear to the present knowledge. However, a coupled ocean-atmosphere mechanism is known to play a significant role in weakening the Indian summer monsoon during the North Atlantic cold spells. In this context, the reorganisation of Hadley circulation and associated pressure system in response to these cold events may lead to changes in the Indian winter monsoon over the equatorial Indian Ocean during northern winters. Thus, this study signifies the need for comprehensive investigations on the seasonal response of tropical atmospheric circulation to diabatic cooling, either as climate model simulations or integrated with real-time data, to unravel the exact mechanism of North Atlantic forcing.

Author contributions

Project conceptualisation and fund acquisition –RC and JR; Geochemical & data analysis and interpretation –KMP; Manuscript writing –KMP and RC with the assistance of all authors; AMS ^{14}C measurements and interpretation – KG and SLL; Project administration and supervision – RC, NR, and SLL; Review and editing – all authors.

Consent for publication

All authors have approved the manuscript and agree with its submission.

Data availability

Materials and additional data related to this paper are available from the corresponding authors upon request.

Funding

ORCID iDs

Rohana Chandrajith [iD] https://orcid.org/0000-0003-3072-5240
Joyanto Routh [iD] https://orcid.org/0000-0001-7184-1593

Supplemental material

Supplemental material for this article is available online.

References

Achyuthan H, Nagasundaram M, Gourlan AT et al. (2014) Mid-Holocene Indian summer monsoon variability off the Andaman Islands, Bay of Bengal. *Quaternary International* 349: 232–244.

Alley R and Agustsdottir A (2005) The 8k event: cause and consequences of a major Holocene abrupt climate change. *Quaternary Science Reviews* 24: 1123–1149.

Baker HS, Mbengue C and Woollings T (2018) Seasonal sensitivity of the Hadley cell and Cross-Hemispheric responses to diabatic heating in an idealized GCM. *Geophysical Research Letters* 45: 2533–2541.

Band S, Yadava MG, Lone MA et al. (2018) High-resolution mid-Holocene Indian summer monsoon recorded in a stalagmite from the Kotumsar Cave, Central India. *Quaternary International* 479: 19–24.

Bhushan R, Sati SP, Rana N et al. (2018) High-resolution millennial and centennial scale Holocene monsoon variability in the higher central Himalayas. *Palaeogeography, Palaeoclimatology, Palaeoecology* 489: 95–104.

Blaauw M and Christen JA (2011) Flexible paleoclimate age-depth models using an autoregressive gamma process. *Bayesian Analysis* 6: 457–474.

Bond G, Kromer B, Beer J et al. (2001) Persistent solar influence on North Atlantic climate during the Holocene. *Science* 294: 2130–2136.

Bond G, Showers W, Cheseby M et al. (1997) A pervasive millennial-scale cycle in North Atlantic Holocene and glacial climates. *Science* 278: 1257–1266.

Caballero R (2007) Role of eddies in the interannual variability of Hadley cell strength. *Geophysical Research Letters* 34: L22705.

Ceppi P and Hartmann DL (2013) On the speed of the eddy-driven jet and the width of the Hadley cell in the Southern Hemisphere. *Journal of Climate* 26: 3450–3465.

Chandrajith R (2020) Geology and Geomorphology. In: Mapa R (ed.) *The Soils of Sri Lanka. World Soils Book Series*. Cham: Springer, pp. 23–34.

Chen H, Xu Z, Lim D et al. (2020) Geochemical records of the provenance and silicate weathering/erosion from the eastern Arabian Sea and their responses to the Indian summer monsoon since the mid-Pleistocene. *Paleoceanography and Paleoclimatology* 35: e2019PA003732.

Clement AC and Peterson LC (2008) Mechanisms of abrupt climate change of the last glacial period. *Reviews of Geophysics* 46: RG4002.

Deplazes G, Lückge A, Peterson LC et al. (2013) Links between tropical rainfall and North Atlantic climate during the last glacial period. *Nature Geoscience* 6: 213–217.

Frierson DMW, Hwang Y-T, Fučkar NS et al. (2013) Contribution of ocean overturning circulation to tropical rainfall peak in the Northern Hemisphere. *Nature Geoscience* 6: 940–944.

Gayantha K, Routh J, Anupama K et al. (2020) Reconstruction of the late Holocene climate and environmental history from North Bolgoda Lake, Sri Lanka, using lipid biomarkers and pollen records. *Journal of Quaternary Science* 35: 514–525.

Gayantha K, Routh J and Chandrajith R (2017) A multi-proxy reconstruction of the late holocene climate evolution in Lake Bolgoda, Sri Lanka. *Palaeogeography, Palaeoclimatology, Palaeoecology* 473: 16–25.

Gupta AK, Anderson DM and Overpeck JT (2003) Abrupt changes in the Asian southwest monsoon during the Holocene and their links to the North Atlantic Ocean. *Nature* 421: 354–357.

Hao T, Liu X, Ogg J et al. (2017) Intensified episodes of East Asian Winter Monsoon during the middle through late holocene driven by North Atlantic cooling events: High-resolution

lignin records from the South Yellow Sea, China. *Earth and Planetary Science Letters* 479: 144–155.

Henry LG, McManus JF, Curry WB et al. (2016) North Atlantic ocean circulation and abrupt climate change during the last glaciation. *Science* 353: 470–474.

Hu B, Yang Z, Zhao M et al. (2012) Grain size records reveal variability of the East Asian winter monsoon since the Middle Holocene in the Central Yellow Sea mud area, China. *Science China Earth Sciences* 55: 1656–1668.

Kabata-Pendias A and Pendias H (1984) *Trace elements in soils and plants*. Boca Raton, FL: CRC Press Inc., .p. 548.

Liu X, Tang D and Ge C (2020b) Distribution and sources of organic carbon, nitrogen and their isotopic composition in surface sediments from the southern Yellow Sea, China. *Marine Pollution Bulletin* 150: 110716.

Liu X, Sun Y, Vandenberghe J et al. (2020a) Centennial- to millennial-scale monsoon changes since the last deglaciation linked to solar activities and North Atlantic cooling. *Climate of the Past* 16: 315–324.

Liu YH, Henderson GM, Hu CY et al. (2013) Links between the East Asian monsoon and North Atlantic climate during the 8,200 year event. *Nature Geoscience* 6: 117–120.

Lone AM, Achyuthan H, Shah RA et al. (2018) Environmental magnetism and heavy metal assemblages in lake bottom sediments, Anchar Lake, Srinagar, NW Himalaya, India. *International Journal of Environmental Health Research* 12: 489–502.

Lückge A, Doose-Rolinski H, Khan AA et al. (2001) Monsoonal variability in the northeastern Arabian Sea during the past 5000years: Geochemical evidence from laminated sediments. *Palaeogeography, Palaeoclimatology, Palaeoecology* 167: 273–286.

Mishra PK, Ankit Y, Gautam PK et al. (2019) Inverse relationship between south-west and north-east monsoon during the late holocene: Geochemical and sedimentological record from Ennamangalam Lake, southern India. *CATENA* 182: 114117.

Mohtadi M, Prange M, Oppo DW et al. (2014) North Atlantic forcing of tropical Indian Ocean climate. *Nature* 509: 76–80.

Ning D, Zhang E, Sun W et al. (2017) Holocene Indian summer monsoon variation inferred from geochemical and grain size records from Lake Ximenglongtan, southwestern China. *Palaeogeography, Palaeoclimatology, Palaeoecology* 487: 260–269.

Pausata FSR, Battisti DS, Nisancioglu KH et al. (2011) Chinese stalagmite δ18O controlled by changes in the Indian monsoon during a simulated Heinrich event. *Nature Geoscience* 4: 474–480.

Previdi M and Liepert BG (2007) Annular modes and Hadley cell expansion under global warming. *Geophysical Research Letters* 34: L22701.

Rajmanickam V, Achyuthan H, Eastoe C et al. (2017) Early-Holocene to present palaeoenvironmental shifts and short climate events from the tropical wetland and lake sediments, Kukkal Lake, southern India: Geochemistry and palynology. *The Holocene* 27: 404–417.

Rashid H, Flower BP, Poore RZ et al. (2007) A ~25ka Indian Ocean monsoon variability record from the Andaman Sea. *Quaternary Science Reviews* 26: 2586–2597.

Rawat S, Gupta AK, Sangode SJ et al. (2015) Late Pleistocene–Holocene vegetation and Indian summer monsoon record from the Lahaul, northwest Himalaya, India. *Quaternary Science Reviews* 114: 167–181.

Reimer PJ, Bard E, Bayliss A et al. (2013) IntCal13 and Marine13 radiocarbon age calibration curves 0–50,000 years cal BP. *Radiocarbon* 55: 1869–1887.

Sagawa T, Kuwae M, Tsuruoka K et al. (2014) Solar forcing of centennial-scale East Asian winter monsoon variability in the

mid- to late Holocene. *Earth and Planetary Science Letters* 395: 124–135.

Silva EIL, Katupotha J, Amarasinghe O et al. (2013) *Lagoons of Sri Lanka: from the origins to the present*. Colombo: Sri Lanka International Water Management Institute (IWMI).

Steinhof A, Altenburg M and Machts H (2017) Sample preparation at the Jena 14C Laboratory. *Radiocarbon* 59: 815–830.

Tierney JE, Pausata FSR and DeMenocal P (2016) Deglacial Indian monsoon failure and North Atlantic stadials linked by Indian Ocean surface cooling. *Nature Geoscience* 9: 46–50.

Wang P, Clemens S, Beaufort L et al. (2005a) Evolution and variability of the Asian monsoon system: State of the art and outstanding issues. *Quaternary Science Reviews* 24: 595–629.

Wang Y, Cheng H, Edwards RL et al. (2005b) The Holocene Asian monsoon: Links to solar changes and North Atlantic climate. *Science* 308: 854–857.

Wen X, Liu Z, Wang S et al. (2016) Correlation and anti-correlation of the East Asian summer and winter monsoons during the last 21,000 years. *Nature Communications* 7: 11999.

Yancheva G, Nowaczyk NR, Mingram J et al. (2007) Influence of the intertropical convergence zone on the East Asian monsoon. *Nature* 445: 74–77.

Yu X, Zhou W, Liu Z et al. (2011) Different patterns of changes in the Asian summer and winter monsoons on the eastern Tibetan Plateau during the Holocene. *The Holocene* 21: 1031–1036.